Microelectronic Engineering 98 (2012) 488–491

Contents lists available at SciVerse ScienceDirect

Microelectronic Engineering

journal homepage: www.elsevier.com/locate/mee

Stress mapping on the porous silicon microcapsules by Raman microscopy

D. Naumenko [a,*], V. Snitka [a], M. Duch [b], N. Torras [b], J. Esteve [b]

[a] Kaunas University of Technology, Kaunas 51369, Lithuania
[b] Instituto de Microelectrónica de Barcelona, Barcelona 08193, Spain

ARTICLE INFO

Article history:
Available online 23 July 2012

Keywords:
Silicon
Polysilicon
Stress
Raman spectroscopy
Microcapsule

ABSTRACT

Silicon micromachined microcapsules have recently been used in biomedical applications as individual in sensing and drug delivery systems due to its biocompatibility and biodegradability properties. Microcapsules micromachining process is quite a complex procedure and to develop a high outcome the process has to be well controlled. One of the important physical characteristics influencing degradation of the microcapsules during the micromachining is a mechanical stresses in the microcapsules. In this work we investigated the stress in polysilicon microcapsules and their crystallinity before and after electrochemical etching process by means of micro-Raman spectroscopy and atomic force microscopy. It was shown that microcapsules fabrication process leads to the appearance of strong mechanical stress (up to 1.74 GPa), at the edges of produced microcapsules which can damage the structures. The combined AFM and Raman investigations confirm the presence of silicon amorphous phase after technological process and allow the stress mapping. We demonstrate a great potential of Raman stress imaging to be used for the testing of silicon microstructures and an improvement of fabrication process.

1. Introduction

Polycrystalline silicon (poly-Si) takes an important role in the modern micro/nano engineering. In particularly, it is a basic material for building blocks in microelectro-mechanical systems (MEMS), and it has also been used to improve the characteristics of MOS, TFT and related devices [1]. Si and poly-Si layers have different characteristics: during and after processing of MEMS devices, mechanical stress is arising in both the functional materials [1–4]. These stresses may be initiated by the disproportion of thermal steps, due to intrinsic mechanical stresses which are inherent in the formation process of the film, or due to the geometry of the nanostructure. Large stresses can also be induced in the substrate near embedded structures such as trenches or holes. Despite the very precise methods developed for the formation of poly-Si layers, the majority of poly-Si structures exhibit a high compressive stress.

Characterization of the intrinsic stresses is of great importance in the poly-Si technology. For application in the MOS devices, stressed films can lead to a high surface state density at the interfaces and in MEMS it causes bending or buckling of suspended structures and may even break poly-Si structures [5].

Assessment of the reliability of MEMS requires accurate characterization of mechanical stresses. Direct measurements of local stresses must often accompany by analytical or numerical models for deformation due to imprecise knowledge of materials properties, inability to predict the magnitudes of intrinsic residual stresses, and to assist in microsystems design [6]. There are many methods for stress evaluation like X-ray diffraction (XRD) and cross-sectional transmission electron microscopy (XTEM) but these techniques are time consuming and lack spatial resolution or are destructive [7].

The Raman spectroscopy is mostly applied in chemical studies as a complementary technique to infrared spectroscopy, giving information on the chemical composition and crystallinity of the sample [8]. However, since the first reports of Anastassakis et al. on the sensitivity of the Raman peak for mechanical stress [9], the technique has been applied more and more for a stress evaluation. The main advantages of Raman technique in this case are that it is non-destructive, fast, has high spatial resolution and high sensitivity for stress measurements [7,10–14].

Microcapsules are promising structures, especially in biomedical applications as drug delivery systems and individual in vitro sensing devices. Thus it is very important to choose a suitable material for its fabrication (non-toxic and biodegradable) and to study its main properties [15,16].

In this paper, we present an evaluation of stress in poly-Si microcapsules by means of micro-Raman spectroscopy and compositional mapping of crystalline, amorphous and poly-Si regions distributions in Si microcapsules fabricated on Si wafers.

2. Experimental section

The microcapsules fabrication process is schematically shown on Fig. 1. 4″ p-type wafers with 0.01 Ω cm of resistivity were used

* Corresponding author.
E-mail addresses: denys.naumenko@ktu.lt (D. Naumenko), vsnitka@ktu.lt (V. Snitka).

0167-9317/$ - see front matter © 2012 Elsevier B.V. All rights reserved.
http://dx.doi.org/10.1016/j.mee.2012.07.089

as a substrate (Fig. 1a) and a 400 nm silicon oxide was thermally grown (Fig. 1b). Then, a photolithographic step and a dry etching were carried out to pattern the silicon oxide layer (Fig. 1c and d). After photoresist removing (Fig. 1e), a silicon isotropic deep reactive ion etching (DRIE) process was performed to form the bottom structures (Fig. 1f). A 200 nm poly-Si layer was deposited and doped in $POCl_3$ atmosphere (Fig. 1g and h). Then the structures were ready for the electrochemical etching (Fig. 1i). The anodization of the silicon was performed in a double cell tank which holds the electrolyte that is a HF-Ethanol (1:1) solution. While the silicon and poly-Si layers are getting porous, the silicon oxide that acts as a sacrificial layer is removed. Different etching conditions have been applied to optimize the pores dimensions and the total silicon oxide removing. Finally, a current of 100 mA/cm^2 density for 40 s was applied to obtain the optimal conditions for a porous poly-Si microcapsules formation and the totally removing the silicon oxides. The structures designed are square microstructures with 3×3 μm^2, homogenously distributed in a 300 μm thick silicon wafer. So, each microstructure is formed by two different parts: a body, which is the main part, and a base, that it has been only designed to easily remove the structure from the substrate.

The SEM images were obtained on FIB Crossbeam 1560XB microscope (Carl Zeiss AG) to control the fabrication and etching processes. To optimize the conditions for total silicon oxide removing FIB milling was used. Stress characteristics and crystallinity of the poly-Si were determined from the Raman measurements on NTEGRA Spectra system (NT-MDT Inc.) on upright configuration (with 100×, 0.95 NA objective) at the excitation wavelength of 632.8 nm and the controlling laser power of 1 mW to avoid temperature effects. The acquisition time was varying between 1 and 10 s. The AFM characterization was obtained in the tapping mode on the same setup using commercial silicon cantilevers NSG11 with a force constant of 5 Nm^{-1}.

Fig. 2 shows SEM images before and after the porosification process (PP). The application of optimal etching conditions, as mentioned above, allows to obtain porous poly-Si particles and to remove totally the silicon oxide from them. It is clearly seen a cavity inside the microparticle after PP (Fig. 2d).

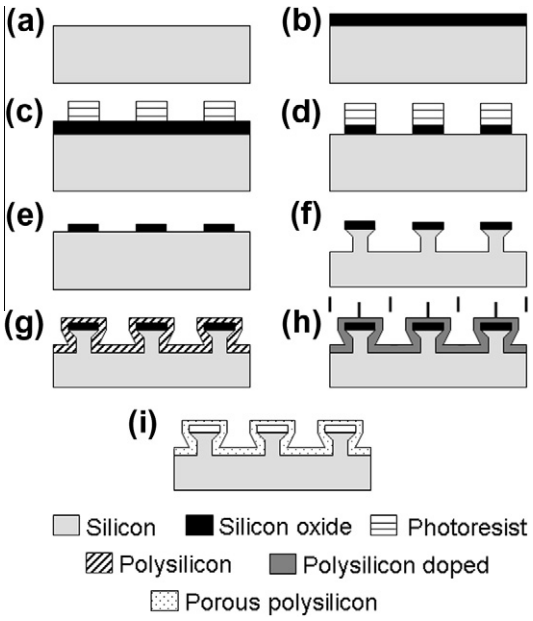

Fig. 1. Fabrication process of polysilicon microcapsules.

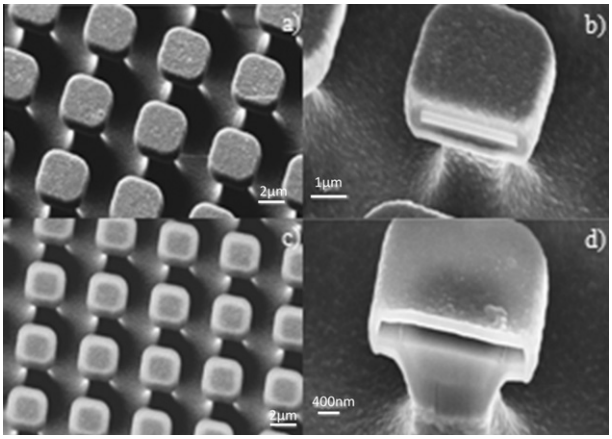

Fig. 2. SEM images of the microcapsules: (a) general view of capsules distribution before electrochemical polysilicon etching, and (b) capsule cross section obtained by FIB; (c) general view of capsules distribution after electrochemical polysilicon etching, and (d) SEM image of a cross section of a porous polysilicon structure obtained by FIB.

3. Results and discussion

The AFM investigations demonstrate the changes in the surface topography of microcapsules after PP (Fig. 3). First of all, the top poly-Si part of the capsule (membrane) is bended after PP (Fig. 3b). The cross-sections of microcapsules obtained by AFM are presented in Fig. 3c. The deflection value of poly-Si membrane reaches up to 200 nm. Naturally, it leads to a high stress in the particles and even their damage, especially on the particle edge (Fig. 3b). AFM investigations of membranes surfaces morphology (Fig. 3d and e) have shown the changes in membrane material crystallinity structure after the electrochemical etching in HF-Ethanol solution. It is seen from Fig. 3d the poly-Si grains and their edges become smoothed (Fig. 3e). It can be explained by the polycrystalline structure amorphization during the etching.

To evaluate a stress value distribution on the microcapsules, it was done a Raman mapping. The Raman spectra were deconvoluted in bands specific the amorphous and crystalline parts by the fitting of spectra with a Gaussian curves [17,18]. The obtained fitting parameters were used to determine the stress level and crystallinity of the samples. 2D or 3D maps of Raman shift, full-width-at-halfmaximum (FWHM) and bands intensity can be analyzed using data collected at different penetration depths of laser beam. Stress free poly-Si exhibits a sharp and strong Raman peak at 520.3 cm^{-1}, corresponding to the optical phonon energy of Si (64 meV) regardless of excitation wavelength. Raman peak position shifts towards the lower wavenumber side when Si is under compressive stress. For stress (σ) calculations it was used the phonon deformation potentials proposed by Anastassakis [19], which gives finally the following equation: $\sigma \approx -435\ \Delta\omega$, where $\Delta\omega$ in cm^{-1}, σ in MPa.

The investigation revealed that the stress is not equally distributed around the perimeter of the capsule. The maximum stress at a level 1.74 GPa was found on the only one side of the microcapsule membrane (Fig. 4). Apparently, it is caused by technological process: the non-uniformity of deposited poly-Si film or thermally grown silicon oxide, for example.

Three dimensional (3D) stress distributions in Si as a result of poly-Si porous particle formation are non-destructively characterized and stress contour maps generated at different depths using a nano-positioning actuator of XYZ scanning stage of micro-Raman spectroscopy system. It was found a similar pattern for stress with the maximal value at the edges (not shown here).

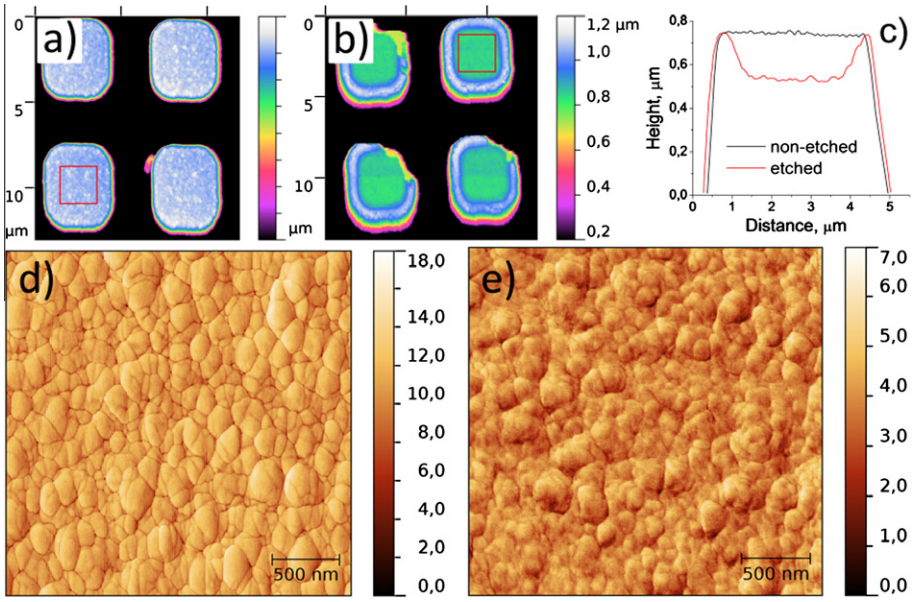

Fig. 3. 15 × 15 µm AFM topography images of non-etched (a) and etched (b) particles and their typical cross-sections (c). 2.5 × 2.5 µm AFM phase images of particles surfaces for non-etched (d) and etched (e) types corresponding to the marked red squares on the images a and b, respectively.

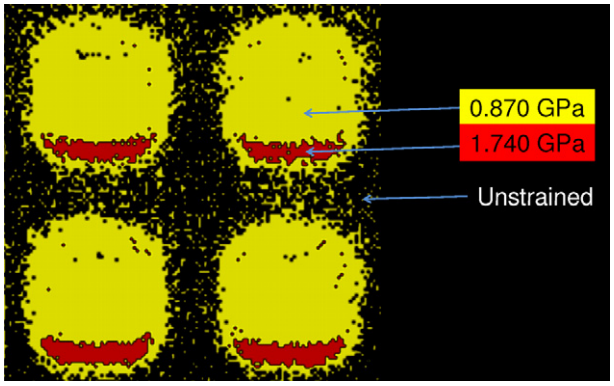

Fig. 4. The typical stress mapping of etched particles surfaces using the model of the phonon deformation potentials of Anastassakis [19].

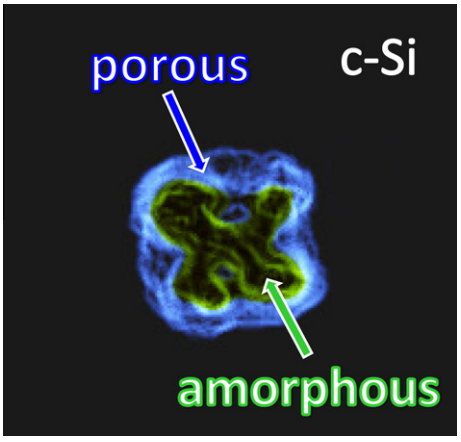

Fig. 5. The compositional Raman mapping of crystalline, amorphous and poly-Si (porous) regions distributions in the etched microcapsules.

The compositional Raman mapping of crystal phases is shown in Fig. 5. It is clearly seen three regions with porous (515–520 cm^{-1}, non-symetric Gaussian fit), amorphous (495–510 cm^{-1}) and crystalline (520 cm^{-1}, symetric Gaussian fit) Si phases.

4. Conclusions

The evaluation of stress in poly-Si microcapsules and their crystallinity before and after electrochemical etching process by combined micro-Raman spectroscopy and atomic force microscopy was done. The Raman mapping of etched microcapsules revealed the maximal value of stress of 1.74 GPa at their edges, value that does affect the viability of the microstructures. It was also shown the changing of poly-Si phase of microcapsules to amorphous one after the electrochemical etching of silicon oxide in HF-Ethanol solution. The combined AFM and Raman investigations of Si microstructures demonstrate a great potential to be used for the stress and crystallinity evaluations and the improving of fabrication process.

Acknowledgments

Authors thank R. Rodriguez for micro-Raman measurements. This work was funded by EU FP7 NANOMAT project: Centre of Excellence in Nanostructured Materials (#229507).

References

[1] M.J. Madou, Fundamentals of Microfabrication, CRC, Boca Raton, FL, 2002.
[2] V.T. Srikar, S.D. Senturia, J. Microelectromech. Syst. 11 (2002) 206–214.
[3] K.-S. Chen, A.A. Ayon, S.M. Spearing, J. Am. Ceram. Soc. 83 (2000) 1476–1484.
[4] K.-S. Chen, A.A. Ayon, X. Zhang, S.M. Spearing, J. Microelectromech. Syst. 11 (2002) 264–275.
[5] C.H. Mastrangelo, Tribol. Lett. 3 (1997) 223–238.
[6] V.T. Srikar, S.M. Spearing, J. Microelectromech. Syst. 12 (2003) 3–10.
[7] I. De Wolf, Semicond. Sci. Technol. 11 (1996) 139–154.
[8] E. Smith, G. Dent, Modern Raman Spectroscopy: A Practical Approach, John Wiley & Sons, 2005.
[9] E. Anastassakis, A. Pinczuk, E. Burstein, F.H. Pollak, M. Cardona, Solid State Commun. 8 (1970) 133–138.
[10] R.C. Teixeira, I. Doi, M.B.P. Zakia, J.A. Diniz, J.W. Swart, Mater. Sci. Eng. B 112 (2004) 160–164.
[11] V.T. Srikar, A.K. Swan, M.S. Unlu, B.B. Goldberg, S.M. Spearing, J. Microelectromech. Syst. 12 (2003) 779–787.
[12] Y. Gogotsi, C. Baek, F. Kirscht, Semicond. Sci. Technol. 14 (1999) 936–944.
[13] M. Holtz, J.C. Carty, W.M. Duncan, Appl. Phys. Lett. 74 (1999) 2008–2010.

[14] M. Bowden, D.J. Gardiner, D. Wood, J. Burdess, A. Harris, J. Hedley, J. Micromech. Microeng. 11 (2001) 7–12.
[15] C. Chiappini, E. Tasciotti, J.R. Fakhoury, D. Fine, L. Pullan, Y.C. Wang, L. Fu, X. Liu, M. Ferrari, Chem. Phys. Chem. 11 (2010) 1029–1035.
[16] E.J. Anglin, L. Cheng, W.R. Freeman, M.J. Sailor, Adv. Drug Deliv. Rev. 60 (2008) 1266–1277.
[17] A.T. Voutsas, M.K. Hatalis, J. Boyce, A. Chiang, J. Appl. Phys. 78 (1995) 6999–7006.
[18] C. Smit, R.A.C.M.M. Van Swaaij, H. Donker, A.M.H.N. Petit, W.M.M. Kessels, M.C.M. van de Sanden, J. Appl. Phys. 94 (2003) 3582–3588.
[19] E. Anastassakis, A. Cantarero, M. Cardona, Phys. Rev. B 41 (1990) 7529–7535.